IOPscience iopscience.iop.org

Home Search Collections Journals About Contact us My IOPscience

Electron–hole drops in silicon with dislocations

This article has been downloaded from IOPscience. Please scroll down to see the full text article.

2002 J. Phys.: Condens. Matter 14 12813

(http://iopscience.iop.org/0953-8984/14/48/320)

View the table of contents for this issue, or go to the journal homepage for more

Download details:
IP Address: 171.66.16.97
The article was downloaded on 18/05/2010 at 19:13

Please note that terms and conditions apply.

INSTITUTE OF PHYSICS PUBLISHING JOURNAL OF PHYSICS: CONDENSED MATTER

J. Phys.: Condens. Matter **14** (2002) 12813–12818 PII: S0953-8984(02)54040-6

Electron–hole drops in silicon with dislocations

N Drozdov and A Fedotov[1]

Belarussian State University, F Skaryna Av. 4, 220050 Minsk, Belarus

E-mail: fedotov@bsu.by

Received 27 September 2002
Published 22 November 2002
Online at stacks.iop.org/JPhysCM/14/12813

Abstract
The processes of electron–hole drop (EHD) formation and migration in silicon crystal containing a significant number of dislocations can have different features as compared with those in dislocation-free crystal. The results of a low-temperature photoluminescence study of EHD in silicon with dislocations presented here show that dislocations in silicon are centres of EHD condensation. In addition to the line for dislocation-free silicon with a maximum at 1.082 eV, the radiative spectrum of EHD in silicon with dislocations contains an additional line with a maximum at 1.078 eV that is due to the appearance of unusual EHD extended or 'spread' along the dislocation axis. The existence of cylindrical EHD on dislocations is confirmed also by the different character of the dependence of the EHD recombination radiation intensity on the excitation intensity and is demonstrated by model calculations.

1. Introduction

The processes of electron–hole drop (EHD) formation and migration in crystals containing a significant number of dislocations differ essentially from those in dislocation-free crystals. This is conditioned by the strong influence of elastic stress fields around dislocations and effective recombination through dislocations on the EHD nucleation. As was theoretically predicted [1], the latter can result in the existence of unusual EHD extended along the dislocations. Also, the dislocations themselves (or accumulations of impurities and point defects around them) can be treated as centres of EHD formation that should result in lowering of the EHD nucleation threshold for a dislocation-containing crystal.

In view of the facts that EHD are very sensitive to elastic stresses and the defect–impurity composition of a crystal and that optical methods enable the recording of very fine changes in the energy characteristics of spectral lines, photoluminescence (PL) measurements of EHD in silicon can be a highly effective tool for studying dislocations *per se* in the material. However,

[1] Author to whom any correspondence should be addressed.

 © 2002 IOP Publishing Ltd Printed in the UK

we could not find any experimental confirmation of the presence of EHD in dislocation-containing crystals.

The present paper is devoted to a low-temperature (4.2 K) PL study of EHD in silicon that enables one to correlate the processes of EHD nucleation, formation and migration in dislocation-containing and dislocation-free crystals.

2. Experimental details

Our experiments were carried out on rectangular phosphorus-doped 800 Ω cm silicon samples with edges measuring $1 \times 2 \times 25$ mm^3. The edges of the rectangles were oriented along $\langle 01\bar{1}\rangle$, $\langle \bar{2}11\rangle$ and $\langle 111\rangle$ directions. The initial density of growth of dislocations was $<10^2$ cm^{-2}. Additional dislocations were introduced into the samples by plastic deformation at 680–730 °C using four-point bending techniques. Using this method of dislocation generation enabled us to produce in the samples three types of region differing in the density and distribution of dislocations. In the central region about 5 mm in diameter, the dislocation density was maximal, N_D^{max} (zone 1). Two regions approximately 7 mm each had gradient distributions of dislocation densities N_D (zones 2). In the regions of the crystal faces (zones 3) N_D was at the level of the initial samples, i.e. $<10^2$ cm^{-2} in our case. The maximal density of dislocations N_D^{max} in zone 1 for each sample was dependent on the temperature of deformation, as well as the value of the bending force and its duration.

The excitation of PL was realized using an Ar- or Kr-ion laser with optical power up to 0.6 W and the possibility of focusing the excitation area down to 0.8 mm in diameter. The samples studied were embedded directly in liquid helium. The probable optical overheating of the sample was controlled by measurement of the spectral width of the free exciton (FE) radiation line. The stimulating (exciting) radiation was modulated with the frequency of 20 Hz. The PL radiation was recorded by a grating monochromator using the photoresistance of Ge:Cu cooled down to 80 K. An electric signal passed through a selectively enhancing tract and, after synchronous detection, was saved as a data file with visualization on a computer monitor.

3. Results

Unfortunately, our attempts to detect the EHD recombination radiation from the central region (zone 1) for samples with high ($\geqslant 10^6$ cm^{-2}) and moderately high ($\sim 10^5$–10^6 cm^{-2}) dislocation densities were unsuccessful. However, EHD radiation and also the recombination radiation of FE and bound excitons (BE) localized on the phosphorus atoms were steadily observed for PL of the facial low-dislocation-density regions (zone 2) for samples with any dislocation density in the central region (zone 1). This may be explained by the impossibility of achieving the EHD condensation threshold in the central zone of the dislocation-containing sample due to high-speed recombination of charge carriers on dislocations.

The measured integral intensities for the particular lines of exciton radiation (both FE and BE), EHD radiation and dislocation recombination radiation (line D_1, $h\nu = 0.82$ eV [2]), when scanning the PL excitation area along zone 2 of the sample with $N_D^{max} = 1 \times 10^6$ cm^{-2}, are presented in figure 1. As shown, the intensities of FE, BE and EHD bands decrease sharply with increasing N_D. This may be due to the high efficiency of exciton capture by dislocations with their subsequent radiative (lines D_1 and D_2 [3]) and non-radiative recombination.

The greatest interest is aroused by the presence of a maximum in the spectrum for the EHD band. In conditions of low excitation, realized in our experiments, this suggests that dislocations in silicon can be considered as centres of the EHD condensation. And the threshold of the free carrier concentration needed for the EHD nucleation is decreased when

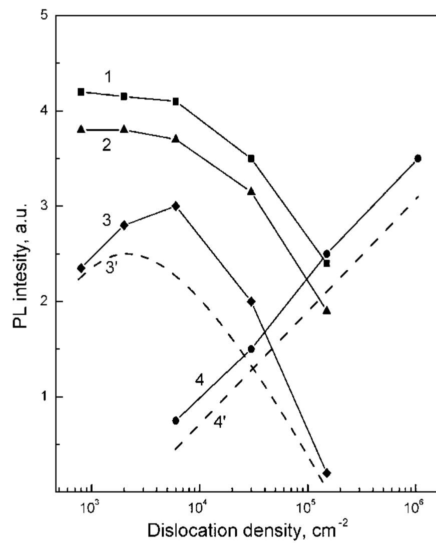

Figure 1. Integral intensity of the particular PL lines versus dislocation density N_D. 1: FE; 2: BE; 3, 3′: EHD; 4, 4′: D_1. Curves 3′ and 4′ correspond to calculated data.

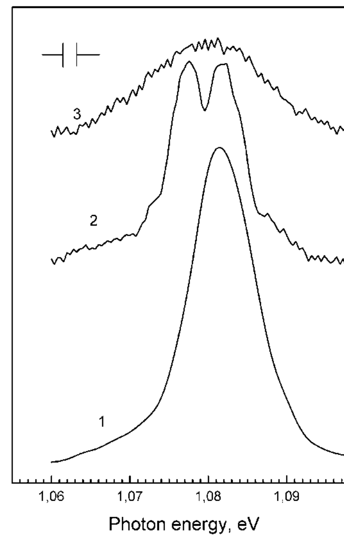

Figure 2. EHD bands in PL spectra for different densities of dislocations N_D. Curves 1, 2 and 3 correspond to the N_D-values 5×10^3, 3×10^4 and 1×10^5 cm^{-2} respectively.

the dislocation density increases. In our experiments the maximal intensity of the EHD line when moving the excitation spot along the sample corresponded to $N_D = (5–10) \times 10^3$ cm^{-2}. Further elevation of N_D led to the predominance of the channels of exciton capture and exciton recombination through dislocations and, hence, to lowering of the exciton bonding rate in EHD.

It should be noted that the spectral contour of the EHD line also changes with increase in the dislocation density. As was shown in [4] and is seen in figure 2 (curve 1) that this contour has a standard form for $N_D < 10^3$ cm^{-2}. As is also seen from figure 2 (curve 2), for $N_D \geqslant 5 \times 10^4$ cm^{-2} the PL spectrum contains the 1.082 eV line along with a band with a maximum at 1.078 eV. For higher values of N_D the intensity of the PL becomes too low, and that prevented us from resolving the fine structure of the EHD band. We believe that the additional component of the spectrum can be attributed to the appearance of the unusual EHD extended, or 'spread', along the dislocation. This 'spreading' is associated with fields of elastic stresses around dislocations leading to an additional possibility for cylindrical EHD nucleation near the dislocation 'core'. A different character of the relationship between the intensity of recombination radiation from drops and the excitation level also confirms the existence of EHD with cylindrical form. EHD, FE and BE lines in the PL spectra for three excitation levels are shown in figure 3. It is seen that for the 1.082 eV component this dependence is close to a cubic one, while it looks practically like a square law for the 1.078 eV line.

It was observed that the EHD radiation and dislocation recombination radiation were polarized. The polarization coefficient P of the dislocation radiation depends on the conditions of plastic deformation of the samples and their subsequent heat treatments. The maximal value of P obtained was about 0.35 for the D_1 line and was not dependent on N_D. The degree of polarization of the EHD radiation increased with the elevation of N_D; however, it remained lower than the polarization of the dislocation recombination radiation. For our samples, the value of P for EHD radiation did not exceed 0.2–0.25. For the initial samples with only grown-in dislocations, no polarization of the dislocation radiation and EHD radiation was detected.

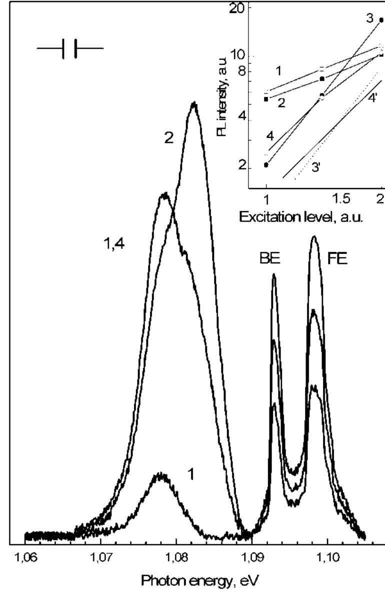

Figure 3. PL spectra in the region of FE, BE and EHD bands for excitation levels in the ratio 1:1.4:2 ($N_D = 3 \times 10^4$ cm^{-2}). Inset: intensities of FE, BE and EHD bands versus excitation level: 1: BE; 2: FE; 3: 1.082 eV EHD band; 4: 1.078 eV EHD band. Curves 3′ and 4′ correspond to calculated data.

4. Discussion

The kinetics of EHD formation and decomposition on dislocations differs from the formation and disintegration kinetics of usual spherical drops. Let us compare the nucleation processes of EHD in their spherical and cylindrical forms. The free Helmholtz energy for the creation of nuclei for a spherical drop is determined as [5]

$$\Delta G = 4\pi R^2\sigma - \tfrac{4}{3}\pi R^3 n_0\, \Delta\mu, \qquad (1)$$

where R is the radius of a drop, σ is the coefficient of surface tension, n_0 is the density of carriers in EHD, $\Delta\mu = kT\,\ln(n_{ex}/n_0)$, n_{ex} is the concentration of FE.

The Helmholtz energy for cylindrical drops on dislocations is as follows:

$$\Delta G = 2\pi R_{cyl}\sigma L - \pi R_{cyl}^2 n_0\, \Delta\mu\, L, \qquad (2)$$

where R_{cyl} is the cylindrical radius of a drop, L is the length of the dislocation in unit volume. In studies of the dislocation contribution to the cylindrical EHD nucleation and formation, it is essential to take into account the influence of elastic stress fields around dislocations on the Helmholtz energy. We used the value of the dislocation component shift for EHD radiation (4 meV) in the framework of the Stoneham model [7], applied earlier by us for analysis of the interaction between dislocations and point defects [8], to establish the conditions for simultaneous existence of spherical and cylindrical drops. Here it was assumed that n_0 has the same value (4×10^{16} cm^3) for spherical and dislocation drops. This balance is possible when the cylindrical radius R_{cyl} of the dislocation EHD is not in excess of about 1–2 μm. For greater R_{cyl} a spherical drop is energetically more favourable.

Earlier we showed [6] that the dislocation recombination radiation for lines D1 and D2 is due to the annihilation of excitons bound with dislocations.

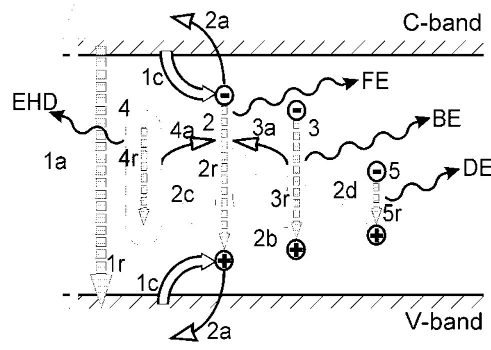

Figure 4. A schematic diagram of the electronic processes in dislocation-containing silicon at low temperatures: 1: for electrons and holes: 1a: electron and hole generation; 1r: electron and hole recombination; 1c: FE formation; 2: for FE: 2a: thermal dissociation of FE; 2b: formation of BE; 2c: formation of EHD; 2d: formation of dislocation-bound excitons; 2r: FE recombination; 3: for BE: 3a: thermal dissociation of BE; 3r: BE recombination; 4: for EHD: 4a: thermal dissociation of EHD; 4r: EHD recombination.

The simultaneous existence of exciton radiation, dislocation radiation and EHD radiation indicates the presence of several competitive channels of exciton capture and recombination in dislocation-containing silicon at low temperatures. The model in figure 4 demonstrates this. The mathematical representation of this model is of the form

$$\frac{\mathrm{d}n}{\mathrm{d}t} = g - \frac{n}{\tau} - \gamma_{ex} n^2 + n_{ex}\alpha_{ex} \exp\left(-\frac{E_{ex}}{kT}\right), \tag{3}$$

$$\frac{\mathrm{d}n_{ex}}{\mathrm{d}t} = \gamma_{ex} n^2 - \frac{n_{ex}}{\tau_{ex}} - n_{ex}\gamma_p(N_p - n_p) - n_{ex}\gamma_d(N_d - n_d) - n_{ex}\alpha_{ex} \exp\left(-\frac{E_{ex}}{kT}\right) + n_p\alpha_p \exp\left(-\frac{E_p}{kT}\right) - n_{ex}\gamma_{ehd} n_{ehd}^{2/3} + n_{ehd}^{2/3}\alpha_{ehd} \exp\left(-\frac{E_{ehd}}{kT}\right), \tag{4}$$

$$\frac{\mathrm{d}n_p}{\mathrm{d}t} = n_{ex}\gamma_p(N_p - n_p) - \frac{n_p}{\tau_p} - n_p\alpha_p \exp\left(-\frac{E_p}{kT}\right), \tag{5}$$

$$\frac{\mathrm{d}n_d}{\mathrm{d}t} = n_{ex}\gamma_d(N_d - n_d) - \frac{n_d}{\tau_d} \tag{6}$$

$$\frac{\mathrm{d}n_{ehd}}{\mathrm{d}t} = n_{ex}\gamma_{ehd} n_{ehd}^{2/3} - \frac{n_{ehd}}{\tau_{ehd}} - n_{ehd}^{2/3}\alpha_{ehd} \exp\left(-\frac{E_{ehd}}{kT}\right). \tag{7}$$

Here $n, n_{ex}, n_p, n_d, n_{ehd}$ are concentrations of free charge carriers, FE, impurity BE, dislocation BE and excitons in EHD, respectively; N_p, N_d are the concentrations of phosphorus atoms and dislocation centres capable of capturing excitons; τ, τ_{ex}, τ_p, τ_d, τ_{ehd} are the proper lifetimes in relation to recombination; E_{ex} is the carrier bonding energy in an exciton; E_p is the bonding energy for an exciton and a phosphorus atom; E_{ehd} is the exciton bonding energy in a drop; γ_{ex}, γ_p, γ_d, γ_{ehd} are the coefficients of free carriers bonding in excitons, excitons bonding with impurities, excitons bonding with dislocations and excitons bonding in EHD; α_{ex}, α_p, α_{ehd} are the coefficients of thermal ejection associated with them.

When constructing this model, the following factors were taken into consideration. The light-generated free charge carriers (electrons and holes) are bound in excitons. FE can be bound with impurities, dislocations and in EHD. Also, recombination of carriers in exciton and thermal dissociation of excitons is possible. For excitons bound to the impurities and those in drops, processes of recombination and dissociation of FE are also possible. For excitons at

dislocations, we can ignore the thermal ejection due to quite large binding energy (the energy shift of the D1 and D2 lines in relation to the FE line is hundreds of millielectron volts).

Equation (7) (see [9]) was deduced from the free Helmholtz energy shown in equation (1) and hence can be applied to the spherical EHD only. Similarly, for the cylindrical EHD on a dislocation, the following equation can be obtained:

$$\frac{\mathrm{d}n^*_{ehd}}{\mathrm{d}t} = n_{ex}\gamma^*_{ehd}n^{*1/2}_{ehd} - \frac{n^*_{ehd}}{\tau^*_{ehd}} - n^{*1/2}_{ehd}\alpha^*_{ehd}\exp\left(-\frac{E^*_{ehd}}{kT}\right). \tag{8}$$

We derived the numerical solution for the system of equations (3)–(8) for the stationary case. The calculated curves were obtained for the following parameters: $T = 4.2$ K; $g = 10^{19}$ cm^{-3} s^{-1}; $\tau = 10^{-3}$ s; $\tau_{ex} = \tau_p = \tau_d = \tau_{ehd} = 10^{-5}$ s; $\gamma_{ex} = 10^2$ cm^3 s^{-1}; $\gamma_p = 10^{-9}$ cm^3 s^{-1}; $\gamma_d = 10^{-11}$ cm^3 s^{-1}; $\gamma_{ehd} = 10^{30}$ cm^2 s^{-1}; $\alpha_{ex} = 10^{15}$ s^{-1}; $\alpha_p = 10^{10}$ s^{-1}; $\alpha_{ehd} = 10^{10}$ s^{-1} cm$^{1/3}$. As seen from figure 1 and the inset in figure 3, this model exhibits not only qualitative but also, in some specific cases, quantitative agreement with the experimental results for the intensities of FE, BE, EHD and D_1, D_2 lines as a function of the temperature, excitation level and dislocation density. However, for closer agreement the processes of exciton diffusion and drift in the vicinity of dislocations should be taken into account.

5. Conclusions

The results obtained show that in dislocation-containing silicon crystals the processes of generation, capture and recombination of free carriers, free and bound on impurities and dislocations excitons and EHD differ essentially from those for the dislocation-free counterparts. A model proposed for the stationary case gives an at least qualitative agreement with the experimental intensity for FE, BE, EHD and D_1, D_2 lines as a function of the temperature, excitation level and dislocation density. To obtain a closer agreement, it is necessary to take into account diffusion and drift of excitons in the vicinity of dislocations.

References

[1] Bozhokin S V *et al* 1981 *Sov. Phys.–JETP* **80** 627
[2] Drozdov N A *et al* 1976 *JETP Lett.* **23** 597
[3] Drozdov N A *et al* 1977 *Phys. Status Solidi* b **83** k137
[4] Martin R W *et al* 1974 *Phys. Status Solidi* b **62** 443
[5] Westervelt R M 1998 *Electron–Hole Drops in Semiconductors* ed K D Jeffris and L V Keldysh (Moscow: Nauka)
[6] Drozdov N A *et al* 1989 *Proc. 5th Int. Conf. on Properties and Structure of Dislocations in Semiconductors (Moscow, March 1986)* p 92
[7] Stoneham A M 1966 *Proc. Phys. Soc.* **89** 909
[8] Drozdov N A *et al* 1988 *Radiat. Eff.* **107** 1
[9] Rice T M 1977 *Solid State Phys.* **32** 1